

## Kinetic chemistry modelling of atmospheric pressure plasma jets

Tomoyuki Murakami

村上朝之

Tokyo Institute of Technology

4259, Nagatsuta, Midori, Yokohama, Kanagawa 226-8503, Japan  
東京工業大学, 〒226-8503 神奈川県横浜市緑区長津田町4259

Atmospheric-pressure plasma jets (APPJs) have been gaining attention because of their great potential in various fields, e.g. surface treatment, environmental remediation and bio-plasma applications. In order to understand the underlying operating principles of such systems and to optimize their performance in applications, it is important to know the chemical kinetics of the reactive multi-species plasma. Recent results on modelling of gas-phase chemical kinetics in low-temperature atmospheric pressure plasma jets operated in an open-air environment are discussed.

## 1. Introduction

Atmospheric-pressure plasma jets (APPJs) have been gaining attention because of their great potential in fabrication of nano-materials or bio-plasma applications. In order to understand the underlying operating principles of such systems and to optimize their performance in applications, it is crucial to determine the evolution of the relevant species' densities and to reveal the underlying reaction chemistry, so that the composition of impacting species can be tailored to a specific application.

## 2. Modeling

A zero-dimensional time-dependent global plasma chemistry model with the extended reaction scheme to describe the complex plasma-induced non-equilibrium chemical network is introduced.

The complex plasma-induced chemistry of both the neutral and ionic compositions in atmospheric pressure He+0.5%O<sub>2</sub> plasmas with humid air impurity is quantitatively revealed using the global model [1,2].

The present global plasma chemical kinetics model and simulation code describes a capacitively-coupled, rf-driven micro-scale APPJ (rf- $\mu$ APPJ) as the exemplar source [3]. This device was developed by Schulz-von der Gathen et al. [4, 5] on the basis of the original concept of Schütze et al. [6] but scaled-down and optimized for optical access. It consists of two plane-parallel stainless-steel electrodes enclosed by quartz windows along each side. One electrode is grounded, and the other is driven at a frequency of 13.56 MHz, using an rf power supply via an impedance matching network. This forms a core plasma channel of 30 mm length and 1 mm  $\times$  1

mm cross section. Considered throughout is a typical feed gas flux of 1 slm, which corresponds to a mean gas flow velocity of 17 m/s and a residence time in the core plasma region of about 2 ms. The gas pressure is 0.1 MPa (atmospheric pressure). The gas temperature in the core plasma region is set to 345 K.

Because of the presence of humid air, the plasma tends to produce significant amounts of reactive species and the plasma-induced chemical reactions are complex. So, here, the extended reaction scheme comprises over 1500 elementary reactions among 65 species.

Table I. Species considered

Neutrals	Carrier gas	He
	Admixture	O <sub>2</sub>
	Humid air	N <sub>2</sub> (78.25%), O <sub>2</sub> (20.97%), CO <sub>2</sub> (0.03%), H <sub>2</sub> O (0.75%)
	Reactive species	He*, He2*, O, O(1D), O(1S), O <sub>2</sub> (1D), O <sub>2</sub> (1S), O <sub>3</sub> , O <sub>2</sub> v <sub>1</sub> , O <sub>2</sub> v <sub>2</sub> , O <sub>2</sub> v <sub>3</sub> , O <sub>2</sub> v <sub>4</sub> , N, N <sub>2</sub> v <sub>1</sub> , N <sub>2</sub> v <sub>2</sub> , N <sub>2</sub> v <sub>3</sub> , N <sub>2</sub> v <sub>4</sub> , N(2D), N(2P), NO, NO <sub>2</sub> , NO <sub>3</sub> , N <sub>2</sub> O, H, OH, HO <sub>2</sub> , H <sub>2</sub> , H <sub>2</sub> O <sub>2</sub> , HNO, HNO <sub>2</sub> , HNO <sub>3</sub>
Ions	Positive	He+, He <sub>2</sub> +, O+, O <sub>2</sub> +, O <sub>4</sub> +, N+, N <sub>2</sub> +, N <sub>4</sub> +, NO+, H <sub>2</sub> O+, H <sub>3</sub> O+, H <sub>3</sub> O+.OH, H <sub>3</sub> O+.H <sub>2</sub> O, O <sub>2</sub> +H <sub>2</sub> O
	Negative	O-, O <sub>2</sub> -, O <sub>3</sub> -, O <sub>4</sub> -, NO-, NO <sub>2</sub> -, NO <sub>3</sub> -, CO <sub>3</sub> -, CO <sub>4</sub> -, O <sub>2</sub> -.H <sub>2</sub> O, NO <sub>2</sub> -.H <sub>2</sub> O, NO <sub>3</sub> -.H <sub>2</sub> O, CO <sub>3</sub> -.H <sub>2</sub> O, CO <sub>4</sub> -.H <sub>2</sub> O
Electrons		Electrons

As discussed in [1,2], the explicit time-dependencies of the electron temperature and the production rate of metastable atomic helium ( $\text{He}^*$ , mostly in the lowest triplet state) in the centre of the plasma bulk, as well as the wall (electrode surface) loss rate of several key ionic species in the core plasma region, are at first obtained from one-dimensional (1D) simulations [3] for a  $\text{He}+0.5\%\text{O}_2$  feed gas without other impurities and are then imposed in the global model. Our approach to employ input parameters from the 1D simulation yields information on the impact of the  $\text{He}^*$  initiated plasma on the associated plasma chemistry. As for the core plasma region, the global model describes the chemical kinetics at the fixed source of the ionisation input, which would most closely correspond to a constant input power in the experiments.

### 3. Results

Figure 1 shows the temporal evolution of pronounced reactive neutral species in both (left-hand side) the core plasma region and (right-hand side) the effluent region of an rf-APPJ. The calculation is conducted with an air fraction  $\text{air}/(\text{He} + 0.5\%\text{O}_2) = 0.025\%$  (humidity of 50%). The O-atom density reaches a value of  $5 \times 10^{15} \text{ cm}^{-3}$  at the exit of the core region then declines rapidly in the afterglow (Fig.1(a)). The maximum  $\text{O}_2(1D)$  density at the jet's nozzle is  $7 \times 10^{15} \text{ cm}^{-3}$ , which monotonically decreases in the afterglow. The  $\text{O}_3$  density, in contrast, gradually increases showing the trend to be saturated. The H and  $\text{HO}_2$  densities decrease in the afterglow (Fig.1(b)). While the OH density increases to reach a peak at around 0.5 ms, and then decreases after 3 ms. The densities of  $\text{H}_2$ ,  $\text{H}_2\text{O}_2$ ,  $\text{HNO}_2$  and  $\text{HNO}_3$  increases in the afterglow. The N-atom density decreases dramatically (Fig.1(c)). The NO,  $\text{NO}_2$ ,  $\text{NO}_3$  densities stay nearly constant in the whole afterglow region. While, the  $\text{N}_2\text{O}$  density increases by a factor of two after 3 ms.

### 4. Summary

In most applications helium-based plasma jets operate in an open-air environment. The presence of humid air in the plasma jet will influence the plasma chemistry and can lead to the production of a broader range of reactive species. The present global model can provide valuable insights into the underlying core and afterglow chemical reaction kinetics of atmospheric-pressure non-thermal plasmas.

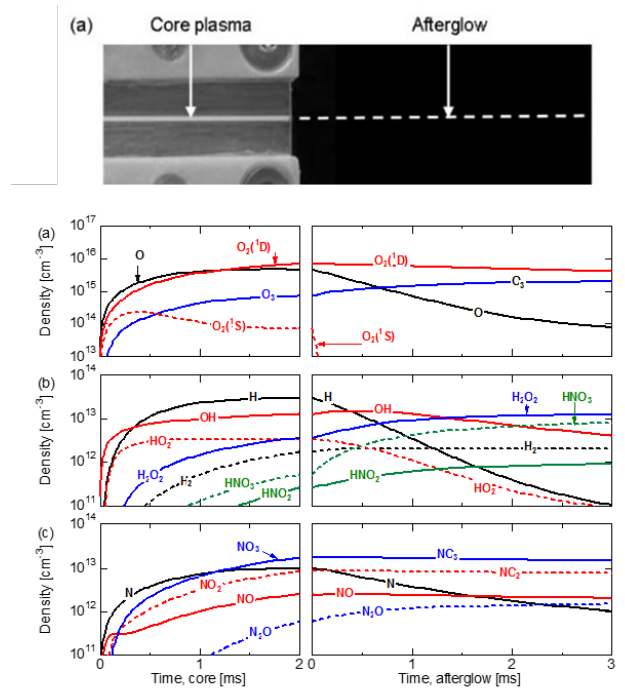


Fig.1. Core and afterglow species in an rf-driven  $\text{He}+\text{O}_2+\text{humid air}$  plasma

### Acknowledgments

This work was supported by MEXT KAKENHI Grant Number 24110704, JSPS KAKENHI Grant Number 24561054, and the UK EPSRC (grant numbers EP/D06337X/1, EP/H003797/1, EP/K018388/1).

### References

- [1] T. Murakami, K. Niemi, T. Gans, D. O'Connell and W. G. Graham: Plasma Sources Sci. Technol. 22 (2013) 015003.
- [2] T. Murakami, K. Niemi, T. Gans, D. O'Connell and W. G. Graham: Plasma Sources Sci. Technol. 22 (2013) 045010.
- [3] K. Niemi, J. Waskoenig, N. Sadeghi, T. Gans and D. O'Connell: Plasma Sources Sci. Technol. 20 (2011) 055005.
- [4] V. Schulz-von der Gathen, V. Buck, T. Gans, N. Knake, K. Niemi, S. Reuter, L. Schaper and J. Winter: Contrib. Plasma Phys. 47 (2007) 510.
- [5] V. Schulz-von der Gathen, L. Schaper, N. Knake, S. Reuter, K. Niemi, T. Gans and J. Winter: J. Phys. D: Appl. Phys. 41 (2008) 194004.
- [6] A. Schütze, J. T. Jeong, S. E. Babayan, J. Park, G. S. Selwyn and R. F. Hicks: IEEE Trans. Plasma Sci. 26 (1998) 1685.
- [7] J. Waskoenig, K. Niemi, N. Knake, L. M. Graham, S. Reuter, V. Schulz-von der Gathen and T. Gans: Plasma Sources Sci. Technol. 19 (2010) 045018.
- [8] J. S. Sousa, K. Niemi, L. J. Cox, Q. Th. Algwari, T. Gans and D. O'Connell: J. Appl. Phys. 109 (2011) 123302.